High Power Indium Phosphide Photonic Integrated Circuit Platform

Hongwei Zhao, Sergio Pinna, Fengqiao Sang, Simone Tommaso Šuran Brunelli,
Larry A Coldren, Jonathan Klamkin
Electrical and Computer Engineering Department, University of California Santa Barbara,
Santa Barbara, CA 93106, USA
Email: hwzhao@ece.ucsb.edu / Phone: (805)8935955

High-power photonic integrated circuits (PICs) are of interest for a variety of applications including microwave photonics, free space optical communications and coherent LiDAR systems [1, 2]. Indium phosphide (InP) is the most advanced platform for high-performance PICs. InP PICs are particularly attractive for free space optical communications, which requires low cost, size, weight and power (CSWaP) [3-5]. In conventional InP PICs, saturation power of semiconductor optical amplifiers (SOAs) is limited by small modal size and high confinement factor (>5%). To improve the SOA saturation power, one approach is to increase the modal size with a flared waveguide, but the large beam dimension in the horizontal direction imposes challenges on the coupling to single-mode fiber [6]. A second approach is to reduce the confinement factor. Slab-coupled optical waveguides (SCOW) with small confinement factor have been investigated for high-power SOAs and lasers. However, it is very challenging to monolithically integrate the SCOW SOAs with other optical elements required for a PIC such as a seed laser and modulator [7]. In this work, we have proposed a novel platform enabling the monolithic integration of low-confinement SOAs with other high-confinement components including a distributed Bragg reflector (DBR) laser and high-speed electro-absorption modulator (EAM).

The epitaxial structure was grown by metal organic chemical vapor deposition (MOCVD) on n-type (001) InP substrates. As shown in Fig. 1(a), two waveguide layers (WG 1 and WG 2) were deposited on the substrate. The lower waveguide layer (WG2) is a low-index dilute waveguide. The active region, on top of the waveguide layers, consists of 5 pairs of indium gallium arsenide phosphide (InGaAsP) quantum wells. The corresponding fundamental TE modes in ridge waveguides are shown in Fig. 1(b) and (c). For a single-ridge waveguide, the ridge width is 3 μm and the vertical etch was stopped above the active region, resulting in a modal area of 3.4 μm^2 and confinement factor of 3.7%. To achieve higher saturation power in SOAs, a larger modal area and lower confinement factor would be preferred. With this epitaxial structure, large modal area can be achieved by engineering the waveguide geometry. As shown in Fig. 1(c), a double-ridge waveguide design enables a modal area up to 11.4 μm^2 while the confinement factor is only 0.35%.

Figure 2 (a) shows the microscope image of fabricated PIC transmitter with the above epitaxial structure. It consists of a DBR laser, a high-speed SOA (SOA 1), an EAM, and a high-power two-section output booster SOA (SOA 2). All components in the transmitter were designed with single-ridge waveguide structure and integrated by quantum well intermixing technique. The bangap of the gain, modulator and passive sections are 1550 nm, 1490 nm and 1450 nm, respectively. The LIV characteristic of the DBR laser is demonstrated in Fig. 2(b), which shows a threshold of 65 mA. Off-chip power versus the current density in the second section of the booster SOA (SOA 2) is shown in Fig. 2(c). The current of the laser gain section, the SOA 1, and the first section of the SOA 2 are 150 mA, 90 mA and 140 mA, respectively. The maximum output power with the above DC biasing is 19.4 dBm (87 mW). The PIC transmitter was solder mounted to ceramic carriers. The P pad of the EAM was wire bonded to a 50-Ω RF feeding transmission line to characterize the high-speed performance. Eye diagrams for NRZ OOK modulation up to 20 Gbps are shown in Fig. 2(d).

With the same epitaxial structure, double-ridge waveguide SOAs were fabricated, which is shown in Fig. 3(a). The length of the SOAs is 4 mm and the waveguides are angled to reduce reflection at the facets. The output optical power of the double-ridge SOA at different input optical power levels is demonstrated in Fig. 3(b). The driving current was increased up to 1 A. The output optical power was measured by a germanium detector, which was placed next to the output facet. With 17-dBm input power, the output power is up to 23.8 dBm (240 mW).

In future work, we will integrate the high-confinement transmitter (Fig. 2(a)) with the low-confinement SOA (Fig. 3(a)). Since they are designed with the same epitaxial structure, it only requires a transition stage between the single-ridge and double-ridge waveguides, where usually a linear width taper is sufficient. Besides, in future measurements with AR coated devices, higher output optical power is expected.

[1] D. O. Caplan, *J. Opt. Fiber Commun*. 4, p. 225-362, 2007. [2] B. Isaac *et al. IEEE Int. Semi. Laser Conf. 2018*, paper MC.7.
[3] H. Zhao *et al. IEEE J. Quant. Elec.,* 24, 6, 2018. [4] H. Zhao *et al., Proc. Adv. Photon. 2018,* paper. ITu4B.6.
[5] V. Rosborough *et al., Proc. Adv. Photon. 2016,* paper ITu2A.3. [6] G. Bendeli *et al., IEEE Photonic Letter*, 3, 1, 1991.
[7] J. J. Plant *et al. IEEE Photon.*Technol. Lett., 17, 4, p.735-737, 2005.

978-1-7281-2111-6/19/$31.00 ©2019 IEEE

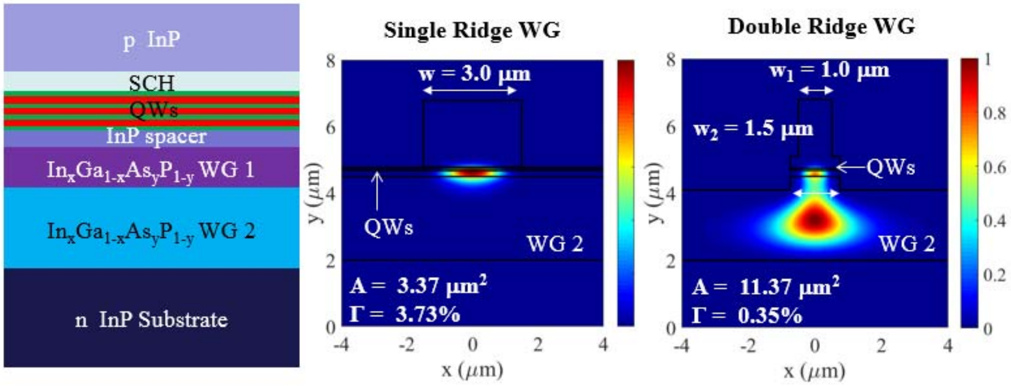

(a) **(b)** **(c)**

Fig. 1. (a) Epitaxial structure (not to scale); (b) Fundamental TE mode in a single-ridge waveguide; (c) Fundamental TE mode in a double-ridge waveguide.

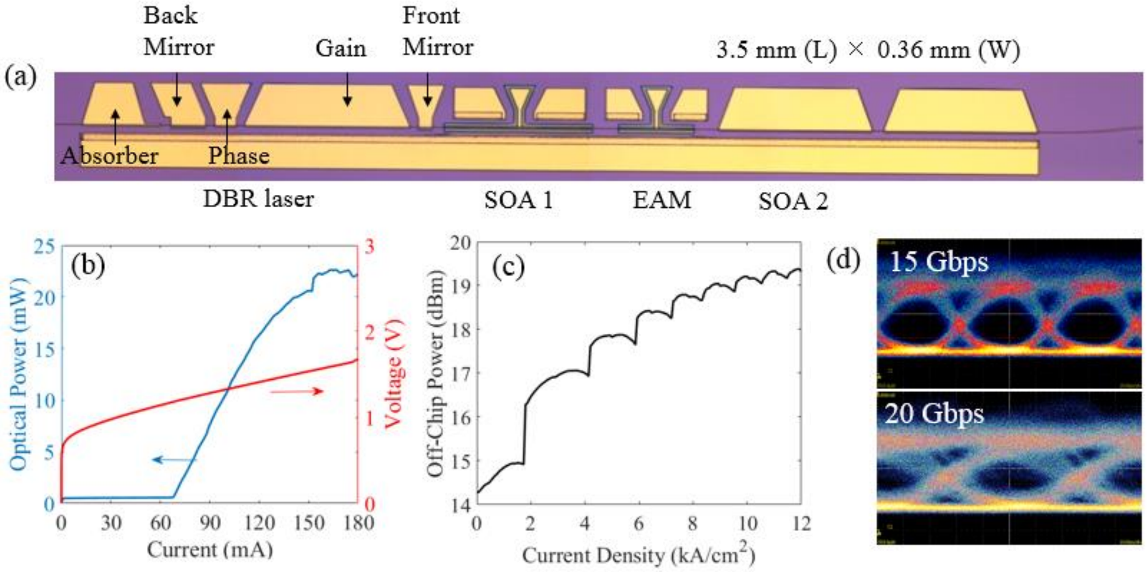

Fig. 2. (a) Microscope image of fabricated InP PIC transmitter consisting of a DBR laser, an electro-absorption modulator and two SOAs, all elements are designed with single-ridge waveguide structure; (b) DBR laser LIV curve (with CW current source); (c) Off-chip optical power of the PIC transmitter versus the current density in the second section of the booster SOA; (d) Eye diagrams with NRZ OOK modulation.

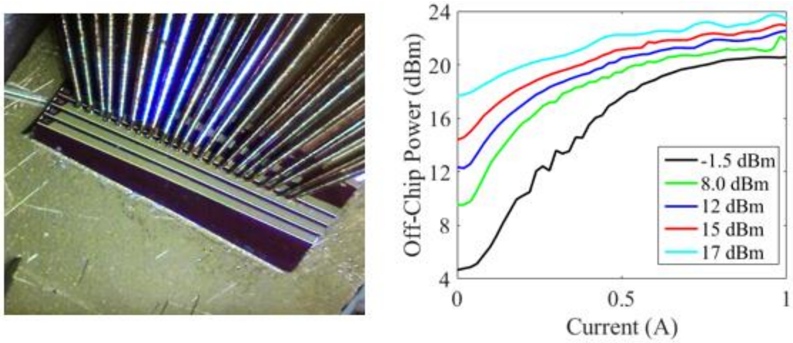

(a) (b)

Fig. 3. (a) Fabricated double-ridge waveguide SOAs (4-mm long); (b) Output optical power of the double-ridge waveguide SOA with different fiber-coupled input power levels.

978-1-7281-2111-6/19/$31.00 ©2019 IEEE